Phorbol 12-Myristate 13-Acetate-Induced Changes in Chicken Enterocytes

Narayan C Rath[1] , Anamika Gupta[2], Rohana Liyanage[3] and Jackson O Lay Jr[3]

[1]USDA, Agricultural Research Service, Poultry Science Center, University of Arkansas, Fayetteville, AR, USA. [2]Department of Poultry Science, Poultry Science Center, University of Arkansas, Fayetteville, AR, USA. [3]Statewide Mass Spectrometry Facility, Department of Chemistry Biochemistry, University of Arkansas, Fayetteville, AR, USA.

ABSTRACT: Increased intestinal epithelial permeability has been linked to many enteric diseases because it allows easy access of microbial pathogens and toxins into the system. In poultry production, the restrictions in the use of antibiotic growth promoters have increased the chances of birds being susceptible to different enteric diseases. Thus, understanding the mechanisms which compromise intestinal function is pertinent. Based on our previous observation which showed the primary chicken enterocytes in culture undergoing dystrophic changes on treatment with phorbol myristate acetate (PMA), we surmised that this model, which appeared to mimic increased intestinal permeability, may help to understand the mechanisms of this problem. As genomic and proteomic changes are associated with many physiological and pathological problems, we were interested to find whether certain proteomic changes underlie the morphological alterations in the enterocytes induced by PMA. We exposed primary enterocyte cultures to a sub-lethal concentration of PMA, extracted the proteins, and analyzed by mass spectrometry for differentially regulated proteins. Our results showed that PMA affected several biological processes which negatively affected their energy metabolism, nuclear activities, and differentially regulated the levels of several stress proteins, chaperon, cytoskeletal, and signal transduction proteins that appear to be relevant in the cause of enterocyte dystrophy. Phorbol myristate acetate-affected signal transduction activities also raise the possibilities of their increased susceptibility to pathogens. The changes in enterocyte integrity can make intestine vulnerable to invasion by microbial pathogens and disrupt gut homeostasis.

KEYWORDS: enterocytes, phorbol ester, proteomic changes, leaky gut

Introduction

Increased intestinal permeability contributes to "leaky-gut," a condition that is linked to several enteric problems because it can permeate microbial pathogens, antigens, and toxins into the system.[1–3] The epithelial integrity prevents bacterial pathogens from entering blood and activate immune system, thereby maintaining a healthy mucosal immunity. In poultry production, the restrictions in the use of "antibiotic growth promoters" have increased the chances of the birds being susceptible to infections and intestinal diseases.[4,5] Hence, understanding how different factors, including microbial pathogens, interact with intestine can help develop products that can improve gut health. The avian enterocyte culture, thus, has potential for screening assays and to study the mechanisms of their interaction with different dietary, microbial, and chemical factors. Previously we observed that the primary chicken enterocytes, when treated with phorbol myristate acetate (PMA), undergo dystrophic changes characterized by cell shrinkage, distended intercellular spaces, and cachectic cellular processes without significant losses of their viabilities.[6] The phorbol esters bind phospholipid membrane receptors of the cells leading to the activation of different proteins and enzymes such as NADPH oxidase, protein kinase C (PKC), and integrins, thus altering cellular adhesion, growth, differentiation, and remodeling.[7] Protein kinase C activation is one of the most studied mechanisms of phorbol esters which activate their membrane recruitment and trigger many cellular responses including inflammation, proliferation as well as cell death, and remodeling.[8,9] We surmised that the dystrophic changes in the enterocytes induced by the action of PMA can be an useful experimental model to study the intestinal permeability changes associated with "leaky-gut" problem. The in vitro observation of the effect of PMA appeared consistent with evidence in the literature where the animals treated with phorbol esters or croton oil, a major source of these esters,[10] disrupt epithelial barrier of the intestine and cause inflammation and cell death.[11–15] On account of the fact that proteomic changes underlie most physio-pathological transformations including morphological and functional alterations, the objective of this study was to determine the proteomic changes in the enterocytes induced by PMA that would cause enterocyte dystrophy.

Methods

Day-old male broiler Cobb 500 chicks, obtained from a local hatchery, were used to harvest intestinal villi, and the enterocytes were dissociated and cultured as described earlier.[6] The animal procedures used were per institutional guidelines. The

villi were treated initially with hyaluronidase followed by trypsin/EDTA and subjected to a density-gradient centrifugation using Histopaque®-1077 (www.sigmaaldrich.com) to separate living cells and cell clusters from the debris. The cells in the interface of density-gradient medium were cultured and expanded in Dulbecco's minimum essential medium (DMEM) containing 10% heat inactivated fetal bovine serum (FBS) IX ITS (insulin, transferrin, and selenite; www.sigmaaldrich.com) and epithelial cell growth supplement (https://www.sciencellonline.com). The enterocytes propagated as individual clusters at the beginning but reached semi-confluence when they were pooled following dissociation with Accumax (www.sigmaaldrich.com) and then replated and expanded in larger flasks. The cells in the third passage were dissociated, counted, and seeded in 12-well plates at the densities of 100 000 cells/mL and grown for 2 days before their treatments with PMA. The cell layers were rinsed twice, each with 1 mL of serum and growth-factor-free culture medium for 5 minutes to deplete exogenous proteins, and then replaced with 1 mL of the same serum-free medium. The treatment cultures were added to 1 µL (500 ng) of PMA dissolved in dimethyl sulfoxide (DMSO), whereas the control cultures received only the DMSO. All assays were done in triplicate, and the changes in the cells were examined microscopically at 24 h to ensure the anticipated morphological changes and photographed. We used replicate cultures, derived from two separate experiments, for mass spectrometric protein analysis.

Proteomic Analyses

After incubation, the cells were removed of supernatant and lysed with 0.5 mL of 4 M guanidine HCl containing 20 mM Na-acetate, pH 6.5, by freeze thaw and repeated trituration. The cell extracts were transferred to fresh tubes, centrifuged at 21 000 g for 10 minutes at 4°C, and the resulting supernatant dialyzed using 5000 MW cut-off Dispo dialyzers (www.spectrumchemical.com) against excess volumes of 25 mM ammonium bicarbonate at 4°C over a 48-hour period with 3 changes. The retentate were transferred to micro-centrifuge tubes and subjected to reduction with 10 mM dithiothreitol (DTT) at 60°C and alkylation with 20 mM iodoacetamide at room temperature for 1 hour, and then digested with 50 ng of MS grade trypsin (www.thermofisher.com) for 24 hours at 37°C.[16,17] The tryptic digests were desalted using Pierce C18 spin columns per manufacturer-suggested protocol. The eluted peptides were dried and resuspended in 0.1% formic acid (FA) for liquid chromatography-mass spectrometry (LC-MS)/MS. Analyses of LC-MS/MS were done using an Agilent 1200 series microflow high-performance liquid chromatography (HPLC) coupled to a Bruker amaZon SL quadrupole ion trap mass spectrometer with a captive spray ionization source. Peptides were separated using a C_{18} capillary column (150 mm × 0.1 mm, 3.5 µm particle size, 300 Å pore size; ZORBAX SB) with 5% to 40% gradients of 0.1% FA (solvent A) and acetonitrile in

0.1% FA (solvent B), and a solvent flow rate of 1.6 µL/min over a 300-minute period each. The captive spray source was operated in a positive ion mode with a dry gas temperature of 150°C, dry nitrogen flow 3 L/min, and capillary voltage of 1500 volts. The data were acquired in the auto MS (n) mode with optimized trapping condition for the ions at m/z 1000. MS scans were performed in an enhanced scanning mode (8100 m/z/s) with collision-induced dissociation and MS/MS fragmentation scans performed automatically for top 10 precursor ions for 1 minute in the ultrascan mode (32 500 m/z/s).[18] The results were based on five replicate samples in each group from two separate experiments.

Data Analyses

Bruker DataAnalysis 4.0 software was used to pick peaks from the LC-MS/MS chromatogram using a default setting as recommended by the manufacturer to create Protein Analysis Results.xml file which were then used for Mascot database search. The parent ion- and fragment ion mass tolerances were both set at 0.6 Da with cysteine carbamidomethylation and methionine oxidation as fixed and variable modifications in Mascot search. Mascot search was carried out against Gallus proteins in UniProt database to identify the proteins in the cell extracts. The peptides from all proteins were identified with 95% confidence limit and reported based on <1% false discovery rate using at least two peptides and one unique peptide from a protein. The uncharacterized Gallus proteins were tentatively identified by their gene sequence similarities. Mascot.dat files were then exported into Scaffold Proteome Software version 4.8 (http://www.proteomesoftware.com) to identify differentially expressed proteins.[19] The quantitative differences were calculated on the basis of 95% confidence limit. The differentially regulated proteins were subjected to functional annotations by gene ontology (GO) terms of proteins using Protein Analysis Through Evolutionary Relationships software (PANTHER; http://pantherdb.org). The differentially expressed proteins were also subjected to STRING protein association network (https://string-db.org) and obtain KEGG pathway associations.

Results

Phorbol myristate acetate treatment produced cellular dystrophy, cachectic changes in the cells, and increased intercellular spaces, while the cells remained attached to the wells (Figure 1). Longer incubation up to 48 hours severely shrunk the cells' widening intercellular spaces, often, detaching cell clusters from the substratum (not shown).

There were a total of 333 proteins consisting of 236 clusters, of which 15 clusters were uniquely present in control and 3 in PMA treated cells (Figure 2; Supplemental Table S1). Quantitative comparison showed upregulation of 24 individual (13 clusters) and downregulation of 63 proteins (51 clusters) by PMA treatment (Figure 2; Table 1).
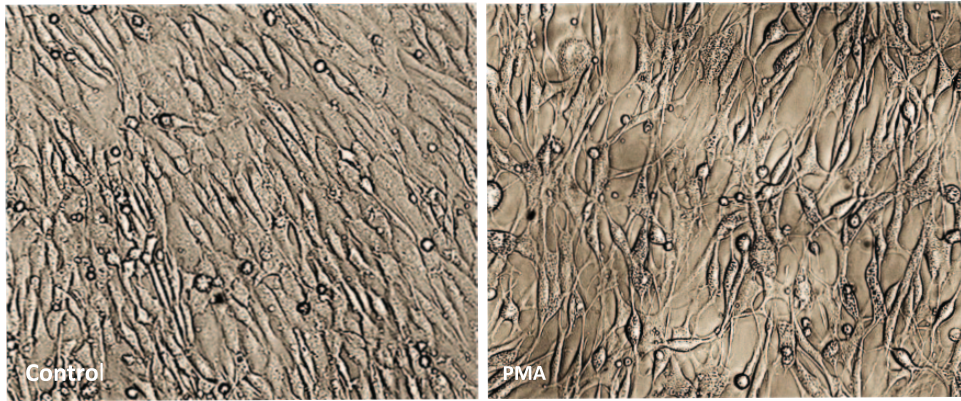
Figure 1. Chicken ileal enterocytes showing morphological changes induced by PMA at 24 hours following treatment (magnification 100×).
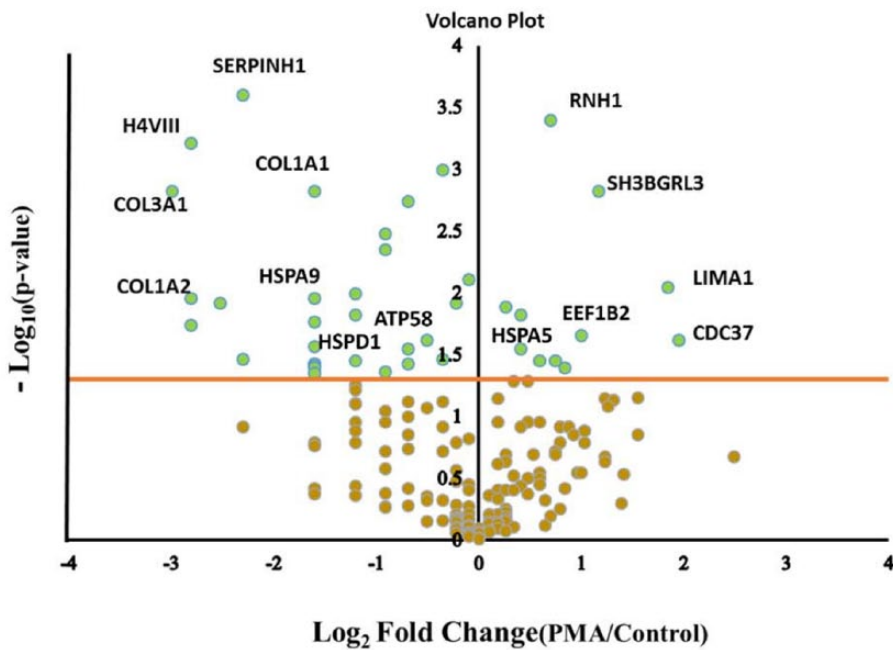

Figure 2. Venn diagrams showing the common and differentially expressed individual proteins and protein clusters and a volcano plot showing down- and upregulated protein clusters.

Table 1. Differentially regulated proteins in the enterocytes by PMA treatment.

PROTEINS	UNIPROT ACCESSION NUMBER	ALTERNATE ID BY GENE	T-TEST (P-VALUE): ($P < .05$)	FOLD CHANGE BY CATEGORY (PMA/C)	COMMON NAME
Downregulated proteins					
Histone H1 OS=Gallus gallus, PE=1, SV=2	H1_CHICK		0.00017	0	Histone
Collagen alpha-1(III) chain (Fragments) OS=Gallus gallus, GN=COL3A1, PE=2, SV=2	CO3A1_CHICK	COL3A1	0.0005	0	Collagen III
Uncharacterized protein OS=Gallus gallus, GN=PHGDH, PE=3, SV=2	E1C7Y3_CHICK	PHGDH	0.0017	0	Phosphoglycerate dehydrogenase
Uncharacterized protein (Fragment) OS=Gallus gallus, GN=PDXK, PE=4, SV=2	F1NKE8_CHICK	PDXK	0.0017	0	Pyridoxal kinase
60S ribosomal protein L6 OS=Gallus gallus, GN=RPL6, PE=2, SV=1	Q8UWG7_CHICK	RPL6	0.002	0	Ribosomal protein L6
Cluster of Histone H1 OS=Gallus gallus, PE=1, SV=2 (H1_CHICK)	H1_CHICK		0.0034	0	Histone
Histone H1.11L OS=Gallus gallus, PE=1, SV=2	H11L_CHICK		0.0034	0	Histone
Uncharacterized protein OS=Gallus gallus, GN=HIST1H111R, PE=3, SV=1	F1NME1_CHICK	HIST1H111R	0.0034	0	Histone
Uncharacterized protein OS=Gallus gallus, GN=ALDH18A1, PE=3, SV=2	E1C8Q3_CHICK	ALDH18A1	0.008	0	Aldehyde dehydrogenase
Cluster of Histone H2B 1/2/3/4/6 OS=Gallus gallus, GN=H2B-I, PE=1, SV=2 (H2B1_CHICK)	H2B1_CHICK	H2B-I	0.01	0	Histone
60S ribosomal protein L7a (Fragment) OS=Gallus gallus, GN=RPL7A, PE=4, SV=1	F2Z4L5_CHICK	RPL7A	0.01	0	Ribosomal protein L7a
Apolipoprotein A-I OS=Gallus gallus, GN=APOA1, PE=1, SV=2	APOA1_CHICK	APOA1	0.015	0	Apolipoprotein
Alpha 1 type IIA collagen OS=Gallus gallus, GN=COL2A1, PE=2, SV=1	Q90W37_CHICK	COL2A1	0.024	0	Collagen I
Cluster of fatty acid synthase OS=Gallus gallus, GN=FASN, PE=1, SV=5 (FAS_CHICK)	FAS_CHICK	FASN	0.024	0	Fatty acid synthase
Uncharacterized protein (Fragment) OS=Gallus gallus, GN=PPA1, PE=4, SV=1	F1NT28_CHICK	PPA1	0.024	0	Pyrophosphatase (inorganic)
Uncharacterized protein OS=Gallus gallus, GN=RPL8, PE=3, SV=2	F1NIX0_CHICK	RPL8	0.024	0	Ribosomal protein L8

Table 1. (Continued)

PROTEINS	UNIPROT ACCESSION NUMBER	ALTERNATE ID BY GENE	T-TEST (P-VALUE): (P<.05)	FOLD CHANGE BY CATEGORY (PMA/C)	COMMON NAME
Uncharacterized protein OS=Gallus gallus, GN=*RPL4*, PE=2, SV=1	Q5ZII1_CHICK	*RPL4*	0.024	0	Ribosomal protein L4
Uncharacterized protein OS=Gallus gallus, GN=*GGA*, PE=4, SV=1	E1BVD1_CHICK	*GGA*	0.024	0	ARF-dependent clathrin
40S ribosomal protein S13 OS=Gallus gallus, GN=*RPS13*, PE=2, SV=3	RS13_CHICK	*RPS13*	0.024	0	Ribosomal protein
GTP-binding nuclear protein Ran OS=Gallus gallus, GN=*RAN*, PE=2, SV=1	RAN_CHICK	*RAN*	0.031	0	GTP-binding nuclear protein Ran
Uncharacterized protein (Fragment) OS=Gallus gallus, GN=*RPL18A*, PE=3, SV=2	F1NPD3_CHICK	*RPL18A*	<0.00010	0	Ribosomal protein L18A
Ribosomal protein L19 OS=Gallus gallus, GN=*RPL19*, PE=3, SV=1	F6RW83_CHICK	*RPL19*	< 0.00010	0	Ribosomal protein
Peptidyl-prolyl cis-trans isomerase (Fragment) OS=Gallus gallus, GN=*PPIB*, PE=3, SV=2	F1NV93_CHICK	*PPIB*	<0.00010	0	Peptidyl-prolyl cis-trans isomerase
Uncharacterized protein OS=Gallus gallus, GN=*RPS14*, PE=2, SV=1	Q5ZHW8_CHICK	*RPS14*	< 0.00010	0	Ribosomal protein S14
Uncharacterized protein OS=Gallus gallus, GN=*RPL14*, PE=4, SV=1	F6R347_CHICK	*RPL14*	< 0.00010	0	Ribosomal protein L14
Cluster of Collagen alpha-1(III) chain (Fragments) OS=Gallus gallus, GN=*COL3A1*, PE=2, SV=2 (CO3A1_CHICK)	CO3A1_CHICK	*COL3A1*	0.0015	0.05	Collagen III
Collagen alpha-2(I) chain OS=Gallus gallus, GN=*COL1A2*, PE=4, SV=1	F1P0H9_CHICK	*COL1A2*	0.00061	0.06	Collagen I
Histone H4 type VIII OS=Gallus gallus, GN=*H4-VIII*, PE=3, SV=3	H48_CHICK	*H4-VIII*	0.011	0.06	Histone
Uncharacterized protein OS=Gallus gallus, GN=*RPS2*, PE=3, SV=1	E1C4M0_CHICK	*RPS2*	0.018	0.06	Ribosomal protein S2
Stress-70 protein, mitochondrial OS=Gallus gallus, GN=*HSPA9*, PE=3, SV=1	F1NZ86_CHICK	*HSPA9*	0.012	0.08	HSP 70
Serpin H1 OS=Gallus gallus, GN=*SERPINH1*, PE=1, SV=2	SERPH_CHICK	*SERPINH1*	0.00025	0.1	Serpin/HSP 47
Keratin, type I cytoskeletal 19 OS=Gallus gallus, GN=*KRT19*, PE=3, SV=1	F1NDN9_CHICK	*KRT19*	0.034	0.1	Cytoskeletal keratin type I
Cluster of Collagen alpha-1(I) chain OS=Gallus gallus, GN=*COL1A1*, PE=1, SV=3 (CO1A1_CHICK)	CO1A1_CHICK	*COL1A1*	0.0015	0.2	Collagen type I

(Continued)

Table 1. (Continued)

PROTEINS	UNIPROT ACCESSION NUMBER	ALTERNATE ID BY GENE	T-TEST (P-VALUE): ($P < .05$)	FOLD CHANGE BY CATEGORY (PMA/C)	COMMON NAME
Uncharacterized protein OS=Gallus gallus, GN=VDAC2, PE=2, SV=1	Q9I9D1_CHICK	VDAC2	0.011	0.2	Voltage-dependent anion channel protein
Cluster of adipocyte fatty acid binding protein OS=Gallus gallus, GN=AFABP, PE=2, SV=2 (Q90X55_CHICK)	Q90X55_CHICK	AFABP	0.017	0.2	Adipocyte fatty acid binding protein
Uncharacterized protein OS=Gallus gallus, GN=FABP4, PE=3, SV=1	F1NDE8_CHICK	FABP4	0.023	0.2	Fatty acid binding protein 4
Glucose-6-phosphate isomerase OS=Gallus gallus, GN=GPI, PE=3, SV=1	F1NIJ6_CHICK	GPI	0.027	0.2	Glucose-6-phosphate isomerase
Citrate synthase OS=Gallus gallus, PE=3, SV=1	R4GLP7_CHICK		0.037	0.2	Citrate synthase
Uncharacterized protein OS=Gallus gallus, GN=TXNDC17, PE=4, SV=1	R4GMD9_CHICK	TXNDC17	0.037	0.2	Thioredoxin domain containing 17
Uncharacterized protein OS=Gallus gallus, GN=RPL12, PE=3, SV=2	E1BTG1_CHICK	RPL12	0.039	0.2	Ribosomal protein L12
Cluster of nucleophosmin (Fragment) OS=Gallus gallus, GN=NPM1, PE=4, SV=2 (F1NVA4_CHICK)	F1NVA4_CHICK	NPM1	0.04	0.2	Nucleophosmin
Uncharacterized protein OS=Gallus gallus, GN=RPL23, PE=3, SV=2	E1BY89_CHICK	RPL23	0.044	0.2	Ribosomal protein L23
Uncharacterized protein (Fragment) OS=Gallus gallus, GN=LOC418169, PE=4, SV=1	F1NT57_CHICK	LOC418169	0.044	0.2	Aldo-keto reductase family 1
L-lactate dehydrogenase B chain OS=Gallus gallus, GN=LDHB, PE=1, SV=3	LDHB_CHICK	LDHB	0.01	0.3	Lactate dehydrogenase
Guanine nucleotide-binding protein subunit beta-2-like 1 OS=Gallus gallus, GN=GNB2L1, PE=2, SV=1	GBLP_CHICK	GNB2L1	0.015	0.3	Guanine nucleotide-binding protein
Uncharacterized protein OS=Gallus gallus, GN=TCEB3, PE=4, SV=2	F1NYL7_CHICK	TCEB3	0.035	0.3	Transcription elongation factor B polypeptide 3
Cluster of elongation factor 1-alpha 1 OS=Gallus gallus, GN=EEF1A, PE=2, SV=1 (EF1A_CHICK)	EF1A_CHICK	EEF1A	0.0033	0.4	Elongation factor
Cluster of Histone H2A-III OS=Gallus gallus, PE=1, SV=2 (H2A3_CHICK)	H2A3_CHICK		0.0044	0.4	Histone
Ras-related protein Rab-14 OS=Gallus gallus, GN=RAB14, PE=2, SV=3	RAB14_CHICK	RAB14	0.0073	0.4	Ras-related protein Rab-14

Table 1. (Continued)

PROTEINS	UNIPROT ACCESSION NUMBER	ALTERNATE ID BY GENE	T-TEST (P-VALUE): ($P<.05$)	FOLD CHANGE BY CATEGORY (PMA/C)	COMMON NAME
Triosephosphate isomerase OS=Gallus gallus, GN=TPI1, PE=1, SV=2	TPIS_CHICK	TPI1	0.043	0.4	Triosephosphate isomerase
60S acidic ribosomal protein P0 OS=Gallus gallus, GN=RPLP0, PE=3, SV=2	F1NB66_CHICK	RPLP0	0.0018	0.5	Ribosomal protein
Histone H2A-III OS=Gallus gallus, PE=1, SV=2	H2A3_CHICK		0.0061	0.5	Histone
60 kDa heat shock protein, mitochondrial OS=Gallus gallus, GN=HSPD1, PE=1, SV=1	CH60_CHICK	HSPD1	0.028	0.5	Heat shock protein (HSP) 60
ATP synthase subunit beta (Fragment) OS=Gallus gallus, GN=ATP5B, PE=3, SV=2	H9L340_CHICK	ATP5B	0.037	0.5	ATP synthase
Cluster of elongation factor 2 (Fragment) OS=Gallus gallus, GN=EEF2, PE=4, SV=2 (F1NFS0_CHICK)	F1NFS0_CHICK	EEF2	0.024	0.6	Elongation factor
Cluster of L-lactate dehydrogenase OS=Gallus gallus, GN=LDHA, PE=3, SV=2 (E1BTT8_CHICK)	E1BTT8_CHICK	LDHA	0.001	0.7	Lactate dehydrogenase
Protein disulfide isomerase A4 OS=Gallus gallus, GN=PDIA4, PE=3, SV=1	F1NDY9_CHICK	PDIA4	0.034	0.7	Protein disulfide isomerase A4
Cluster of alpha-enolase OS=Gallus gallus, GN=ENO1, PE=3, SV=2 (F1NZ78_CHICK)	F1NZ78_CHICK	ENO1	0.012	0.8	Enolase
Nonmuscle myosin heavy chain OS=Gallus gallus, PE=2, SV=1	Q789A4_CHICK		0.042	0.8	Nonmuscle myosin
40S ribosomal protein SA OS=Gallus gallus, GN=RPSA, PE=3, SV=1	RSSA_CHICK	RPSA	0.045	0.8	Ribosomal protein
Cluster of beta-actin (Fragment) OS=Gallus gallus, GN=BACT, PE=2, SV=1 (G8HUH5_CHICK)	G8HUH5_CHICK	BACT	0.0077	0.9	Actin
Actin, cytoplasmic 1 OS=Gallus gallus, GN=ACTB, PE=1, SV=1	ACTB_CHICK	ACTB	0.019	0.9	Actin
Upregulated proteins					
Actin, cytoplasmic 2 OS=Gallus gallus, GN=ACTG1, PE=1, SV=1	ACTG_CHICK	ACTG1	0.019	0.9	Actin
Uncharacterized protein OS=Gallus gallus, GN=CKAP4, PE=4, SV=2	F1P360_CHICK	CKAP4	0.013	1.3	Cytoskeleton associated protein 4

(Continued)

Table 1. (Continued)

PROTEINS	UNIPROT ACCESSION NUMBER	ALTERNATE ID BY GENE	T-TEST (P-VALUE): (P<.05)	FOLD CHANGE BY CATEGORY (PMA/C)	COMMON NAME
14-3-3 protein beta/alpha OS=Gallus gallus, GN=YWHAB, PE=2, SV=1	1433B_CHICK	YWHAB	0.025	1.3	14-3-3 protein alpha
Uncharacterized protein (Fragment) OS=Gallus gallus, GN=KRT8, PE=3, SV=2	H9KZP2_CHICK	KRT8	0.039	1.3	14-3-3 protein
14-3-3 protein gamma OS=Gallus gallus, GN=YWHAG, PE=1, SV=1	1433G_CHICK	YWHAG	0.04	1.3	14-3-3 protein gamma
Uncharacterized protein OS=Gallus gallus, GN=KRT3, PE=3, SV=1	R4GGI4_CHICK	KRT3	0.043	1.3	Keratin 3
Uncharacterized protein OS=Gallus gallus, GN=LOC426897, PE=3, SV=2	H9KZP4_CHICK	LOC426897	0.0052	1.4	Keratin type II
Uncharacterized protein OS=Gallus gallus, GN=FLNB, PE=4, SV=2	F1N8D4_CHICK	FLNB	0.0066	1.5	Filamin
78 kDa glucose-regulated protein OS=Gallus gallus, GN=HSPA5, PE=1, SV=1	GRP78_CHICK	HSPA5	0.015	1.5	GRP-78/HSP
Cluster of 14-3-3 protein theta OS=Gallus gallus, GN=YWHAQ, PE=1, SV=1 (1433T_CHICK)	1433T_CHICK [8]	YWHAQ	0.028	1.5	14-3-3 protein theta
Vimentin OS=Gallus gallus, GN=VIM, PE=3, SV=1	F1NJ08_CHICK	VIM	0.025	1.8	Vimentin
Cluster of uncharacterized protein OS=Gallus gallus, GN=CLTA, PE=2, SV=1 (Q5ZHR7_CHICK)	Q5ZHR7_CHICK	CLTA	0.035	1.8	Clathrin
Uncharacterized protein OS=Gallus gallus, GN=RNH1, PE=1, SV=1	Q5ZIY8_CHICK	RNH1	0.0004	2	Ribonuclease inhibitor
Desmin (Fragment) OS=Gallus gallus, PE=2, SV=1	O73665_CHICK		0.0089	2	Desmin
Desmin OS=Gallus gallus, GN=DES, PE=1, SV=1	DESM_CHICK	DES	0.0089	2	Desmin
Uncharacterized protein OS=Gallus gallus, GN=EEF1D, PE=3, SV=2	E1BZG4_CHICK	EEF1D	0.035	2.1	Elongation factor delta
Protein disulfide isomerase A3 OS=Gallus gallus, GN=PDIA3, PE=2, SV=1	PDIA3_CHICK	PDIA3	0.04	2.3	Protein disulfide isomerase A3
Uncharacterized protein OS=Gallus gallus, GN=EEF1B2, PE=3, SV=1	F1NYA9_CHICK	EEF1B2	0.022	2.7	Elongation factor 1-beta

Table 1. (Continued)

PROTEINS	UNIPROT ACCESSION NUMBER	ALTERNATE ID BY GENE	T-TEST (P-VALUE); (P < .05)	FOLD CHANGE BY CATEGORY (PMA/C)	COMMON NAME
SH3 domain-binding glutamic acid-rich-like protein OS=Gallus gallus, GN=*SH3BGRL3*, PE=3, SV=1	E1C8Z5_CHICK	*SH3BGRL3*	0.0015	3.2	SH3 domain-binding glutamic acid-rich-like protein
Uncharacterized protein OS=Gallus gallus, GN=*LIMA1*, PE=4, SV=2	H9KZD7_CHICK	*LIMA1*	0.0089	6.3	LIM domain and actin binding protein
Cluster of HSP 90 co-chaperone Cdc37 OS=Gallus gallus, GN=*CDC37*, PE=2, SV=1 (CDC37_CHICK)	CDC37_CHICK	*CDC37*	0.024	7	Heat shock protein (HSP) 90 co-chaperon
Uncharacterized protein OS=Gallus gallus, PE=3, SV=2	H9L1C1_CHICK		0.00016	INF	Intermediate filament
Cluster of uncharacterized protein OS=Gallus gallus, PE=3, SV=2 (H9L1C1_CHICK)	H9L1C1_CHICK		0.00055	INF	Intermediate filament
Tumor necrosis factor-inducible protein 6 OS=Gallus gallus, GN=*TNFIP6*, PE=2, SV=1	Q155F6_CHICK	*TNFIP6*	0.0095	INF	TNF alpha induced protein 6
Rous sarcoma virus transcription enhancer factor II OS=Gallus gallus, PE=2, SV=1	Q90650_CHICK		0.028	INF	Rous sarcoma virus transcription enhancer factor

There were 10 biological processes affected by PMA, of which 8 were common to both groups although the proteins included in each of these processes were different (Table 2). Table 3 shows the KEGG pathways affected by PMA. There were 12 pathways downregulated and 3 pathways upregulated by PMA treatment. The adhesion functions of the cells were downregulated in PMA-treated cells indicated by the reduction in the levels of two collagen proteins. The downregulated proteins largely belonged to cellular and metabolic processes that included enzyme proteins associated with energy metabolisms such as alpha enolase (*ENO1*), ATP synthase (*ATP5B*), aldehyde dehydrogenase (*ALDH18A1*), phosphoglycerate dehydrogenase (*PHGDH*), triose phosphate isomerase (*TPI1*), lactate dehydrogenase (*LDHA, LDHB*), ATP synthase (*ATP5B*), glucose phosphate isomerase (*GPI*), and fatty acid metabolism and transport-related proteins (fatty acid synthase [*FASN*], apolipoprotein A1 [*APOA1*], and fatty acid binding proteins [*AFABP*]). Several ribosomal proteins and DNA replication and interactive proteins such as elongation factors (*EEF1A, EEF2*), histones (*H4-VIII, H2B-I*), nucleophosmin (*NPM1*), and cytoskeletal proteins (*ACTB, ACTG1*), nonmuscle myosin, and cytokeratin proteins were affected by PMA. Heat shock proteins (*HSP*) such as the HSPs 47(*SERPINH1*), 60 *(HSPD1*), and a mitochondrial stress protein 70 (*HSPA9*) were downregulated on PMA treatment, and HSP 90 co-chaperon (*CDC37*) and a 78 kDa glucose regulated protein (*HSPA5*) were upregulated (Tables 1 and 2). Other upregulated proteins in PMA-treated enterocytes included certain cytoskeletal and structural proteins such as the intermediate-sized filament proteins, vimentin, and keratins, and two or more signal transduction proteins, a clathrin light chain A and a Rous sarcoma virus transcription enhancer factor II (Table 1). Figure 3 shows the number of regulated proteins under different biological processes although all of the regulated Gallus proteins with putative biological functions (Table 1) were not accounted in the chart.

Discussion

Our results show that PMA exerts an anti-anabolic effect on enterocytes, downregulating several proteins which affect different biological processes. Many of the proteins identified were associated with energy metabolism, carbon metabolism, nuclear, signal transduction, cytoskeletal homeostasis, and cell adhesion functions. The downregulation of glycolytic and energy metabolism-associated enzymes such as ATP- and citrate-synthases, glucose 6-phosphate isomerase, and several oxido-reductase enzymes (phosphoglycerate-, aldehyde-, and lactate dehydrogenase, aldo-keto reductase, and thioredoxin domain-containing protein 17 [*TXNDC17*]) indicate diminished mitochondrial activities which were also further evident from the decreased levels of fat metabolism-related proteins. The fat metabolism-associated proteins such as fatty acid synthase, fatty acid binding protein (FABP), and apolipoproteins

Table 2. GO-annotated proteins associated with different biological processes.

| FUNCTIONAL ANNOTATIONS	DOWNREGULATED PROTEINS	UPREGULATED PROTEINS
Biological adhesion	*COL1A2* (collagen alpha-2(I) chain), *COL3A1* (collagen alpha-1(III) chain)	–
Biological regulation	*RAB14* (Ras-related protein Rab-14), *PDIA4* (protein disulfide isomerase A4), *APOA1* (apolipoprotein A-I)	*CDC37* (HSP 90 co-chaperone Cdc37), *HSPA5* (78 kDa glucose-regulated protein), *PDIA3* (protein disulfide isomerase A3)
Cellular component organization or biogenesis	*RAN* (GTP-binding nuclear protein Ran), *HSPD1* (60 kDa heat shock protein, mitochondrial), *COL1A2* (collagen alpha-2(I) chain), *RPS14* (40S ribosomal protein SA), *COL3A1* (collagen alpha-1(III) chain), *NPM1* (nucleophosmin), *RPSA* (ribosomal protein SA), *RPL12* (60S ribosomal proteins L12), *RAB14* (Ras-related protein Rab-14), *ACTB* (actin, cytoplasmic 1), *RPL7A* (40S ribosomal protein L7A), *H2B-I* (histone H2B), *APOA1* (apolipoprotein A-I), *RPL6* (60S ribosomal proteins L6), *RPL14* (ribosomal protein L14)	*LIMA1* (LIM domain and actin binding protein 1), *CLTA* (clathrin light chain A)
Cellular process	*RAN* (GTP-binding nuclear protein Ran, *EEF2* (elongation factor 2), *HSPD1* (60 kDa heat shock protein, mitochondrial), *COL1A2* (collagen alpha-2(I) chain), *RPS14* (ribosomal protein S2), *HSPA9* (HSP 70), *COL3A1* (collagen alpha-1(III) chain), *NPM1* (nucleophosmin), *RPSA* (40S ribosomal protein SA), *RPL8* (60S ribosomal protein L8), *PHGDH* (D-3-phosphoglycerate dehydrogenase), *RPL12* (60S ribosomal protein L12), *RAB14* (Ras-related protein Rab-14), *ACTG1, ACTB* (actin, cytoplasmic 1 and 2), *RPL7A, H2B-I* (Histone H2B), *PDIA4* (protein disulfide isomerase A4), *RPS2, PDXK* (pyridoxal kinase), *APOA1* (apolipoprotein A-I), *EEF1A* (elongation factor 1-alpha 1), *RPL6* (ribosomal protein L6), *RPLP0* (60S acidic ribosomal protein P0), *TPI1* (triosephosphate isomerase)	*LIMA1* (LIM domain and actin binding protein), *CDC37* (heat shock protein90 co-chaperon), *HSPA5, YWHAG* (14-3-3 protein gamma), *YWHAQ* (14-3-3 protein theta), *CLTA* (clathrin light chain A), *YWHAB* (14-3-3 protein beta/alpha), *PDIA3* (protein disulfide isomerase A3)
Developmental process	*FABP4* (fatty acid binding protein), *PDIA4* (protein disulfide isomerase A4), *APOA1* (apolipoprotein A-I)	*PDIA3* (protein disulfide isomerase A3)
Immune system process	*COL1A2* (collagen alpha-2(I) chain), *COL3A1* (collagen alpha-1(III) chain)	*RNH1*(ribonuclease inhibitor)
Localization	*RAN* (GTP-binding nuclear protein Ran), *RPSA* (40S ribosomal protein SA), *VDAC2* (voltage-dependent anion selective channel protein 2), *RAB14, ACTG1, ACTB* (actins), *APOA1* (apolipoprotein A-I)	*CLTA* (clathrin light chain A)
Metabolic process	*RAN* (GTP-binding nuclear protein Ran), *EEF1A* (elongation factor 1 alpha 1), *EEF2* (elongation factor 2), *HSPD1* (60 kDa heat shock protein, mitochondrial), *RS14* (40S ribosomal protein S14), *HSPA9* (mitochondrial stress protein 70), *LDHB* (L-lactate dehydrogenase B chain), *RPSA* (40S ribosomal protein SA), *GNB2L1* (receptor of activated protein C kinase 1), *GPI* (glucose-6-phosphate isomerase), *RPL8* (ribosomal protein L8), *PHGDH* (D-3-phosphoglycerate dehydrogenase), *RAB14* (Ras-related protein Rab-14), *RPL7A* (60S ribosomal protein L7a), *H2B1* (histone H2B 1/2/3/4/6), *RPS2* (ribosomal protein S2), *PDXK* (pyridoxal kinase), *ENO1* (alpha-enolase), *APOAI* (apolipoprotein A-I), *PPAI* (inorganic pyrophosphatase), *FASN* (fatty acid synthase), *ATP5B* (ATP synthase subunit beta), *RPL6* (ribosomal protein L6), *RPLP0* (60S acidic ribosomal protein P0), *TPI1* (triose phosphate isomerase), *LDHA* (lactate dehydrogenase A chain)	*CDC37* (HSP 90 co-chaperone Cdc37), *HSPA5* (78 kDa glucose-regulated protein), *RNH1*(ribonuclease inhibitor)
Multicellular organismal process	*APOA1* (apolipoprotein A-I)	–
Response to stimulus	*HSPA9* (Stress protein 70), *GNB2L1* (receptor of activated protein C kinase 1), *RAB14* (Ras-related protein Rab-14), *PDIA4* (protein disulfide-isomerase A4), *APOA1* (apolipoprotein A-I)	*HSPA5* (78 kDa glucose-regulated protein), *RNH1*(ribonuclease inhibitor), *PDIA3* (protein disulfide-isomerase A3, nucleic acid binding transcription factor)
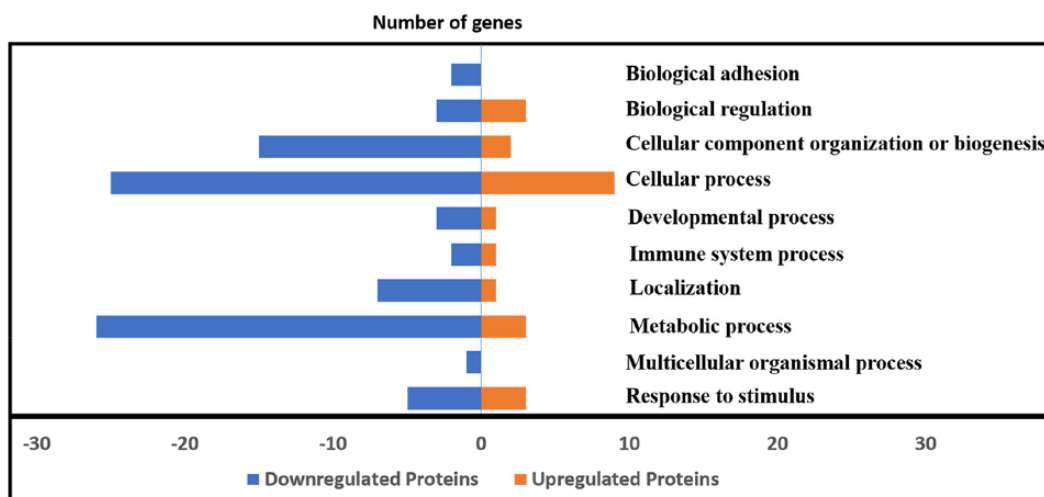
Figure 3. Phorbol myristate acetate-induced down- and upregulated proteins in different biological processes.

Table 3. KEGG pathways affected by PMA treatment.

NO.	PATHWAY ID	PATHWAY DESCRIPTION	COUNT IN GENE SET	FALSE DISCOVERY RATE
Downregulated pathways				
1	03010	Ribosome	14	1.37^{e-17}
2	00010	Glycolysis/gluconeogenesis	5	$1.54^{e-0.05}$
3	01120	Microbial metabolism in diverse environments	6	$6.01^{e-0.05}$
4	01230	Biosynthesis of amino acids	4	0.000701
5	01200	Carbon metabolism	4	0.00317
6	00620	Pyruvate metabolism	3	0.00443
7	01100	Metabolic pathways	10	0.0116
8	03018	RNA degradation	3	0.0164
9	04512	ECM-receptor interaction	3	0.0238
10	04510	Focal adhesion	4	0.0301
11	00051	Fructose and mannose metabolism	2	0.0444
12	00640	Propanoate metabolism	2	0.0444
Upregulated pathways				
1	04110	Cell cycle	3	0.0121
2	04114	Oocyte meiosis	3	0.0121
3	04141	Protein processing in endoplasmic reticulum	3	0.0199

help not only in energy production but also their transportation along with other lipophilic substances such as cholesterol and triglycerides thereby playing key roles in membrane biosynthesis and signaling functions.[20–23] Intestinal tissues constitutively produce FABPs which transport dietary lipids and fatty acids.[24–27] Decreased levels of both FABP and ApoA1 in PMA-treated enterocytes suggest decreased lipid metabolism and their transport that can affect membrane biosynthesis and

remodeling. Phorbol myristate acetate was shown to induce transcriptional suppression of ApoA4 in human hepatic and intestinal cells.[28] Song et al[29] reported the negative effects of phorbol on membrane remodeling based on their studies with human intestinal epithelial cells. Both nuclear and nucleolar functions of enterocytes were also suppressed by PMA which were evidenced by the decrease in the levels of several ribosomal proteins, histone, elongation factor, and nucleophosmin

proteins that are involved in transcription, translational activities, ribosome biogenesis, and degradation. Phorbol myristate acetate also affected both protein maturation and degradation functions indicated by differential changes in HSPs and other chaperon proteins such as peptidyl prolyl cis-trans isomerase (PPIB), thioredoxin domain containing 17, and protein disulfide isomerase (PDIA) family of proteins.[30] The chaperon proteins, particularly the HSPs, are stress proteins that are involved in a variety of functions which include peptide translocation, folding, stabilization, and the degradation of misfolded proteins.[31–33] The HSPs protect the cells against apoptosis and have been implicated in some gastrointestinal diseases.[34–36] HSPs appeared to be differentially regulated by PMA. The HSPs 90, GRP-78, and PDIA3 were upregulated by PMA, the HSPs 47 and 60, and PPIB, whereas PDIA4 were downregulated on PMA treatment. The differential regulations of these stress proteins in the enterocytes are not understood but reciprocal regulations of different stress proteins such as GRP 78 and HSP 70 have been observed in other cells.[37] In certain neurodegenerative diseases, the HSPs 90 and 70 have been shown to have opposing roles on the stability of their respective interacting proteins and their proteosomal degradations.[38] HSPs help maintain intestinal integrity and provide defense against epithelial permeability and their decreased expressions have been reported in conditions that increase gut permeability.[39,40] HSP 47 (*SERPINH1*), which decreased in PMA-treated enterocytes, has been implicated in the etiology of intestinal fibrosis in experimentally induced colitis.[41] Because fibrosis is a condition that relates to the overproduction and deposition of collagens,[42] a decreased expression of HSP 47 in PMA-treated enterocytes, along with the decrease in collagen content, observed in this study seems consistent.

Phorbol myristate acetate also induced differential changes in several cytoskeletal and structural proteins which affect extracellular matrices (ECMs)-receptor interactions and focal adhesion of cells. These included actin, nonmuscle myosin, and keratin 19, all of which were downregulated whereas some others, particularly the intermediate filament-associated proteins, and desmin, and vimentin were upregulated along with keratins 3 and 8. The relationship and the differential regulation of different cytoskeletal proteins are not understood, but it can be related to their metabolic dynamics such as their turnover rates. The dysregulations of cytoskeletal proteins and the adhesion of the cells to their ECM are known to affect their morphology and survival. Activation of PKC affect cell polarization also causes their morphological changes through mechanisms regulating actin cytoskeleton and other stress fibers.[43–45] Similarly, the collagens which are an important component of ECM play significant role in cell-matrix interactions and influence cell attachment and their spreading, and contribute to their phenotypes.[46] Both type I and type III collagens were significantly downregulated in PMA-treated enterocytes. Although there are no data of enterocytes producing collagens, there are many reports of different epithelial cells producing collagens.[47–50] In addition, the PMA-treated enterocytes showed a downregulation in protein named RPSA which is a receptor for laminin present in ECM that facilitates cell adhesion.[51] Taken together, it appears that the changes in cytoskeletal proteins along with the decrease in their collagen production likely affect their spreading and dystrophic changes in the enterocytes.

Phorbol myristate acetate also affected signaling function proteins indicated by the reductions in the level of a mitochondrial, voltage-dependent, anion-selective channel protein 2 that is responsible for ATP channeling and a GTP binding RAS-related nuclear proteins which contribute to the nuclear activities of the cells. Similarly, there were other signal transduction proteins that were upregulated in the enterocytes on PMA treatment. These were three 14-3-3 proteins—beta/alpha, theta, and gamma—which bind to different kinases, phosphatases, and transmembrane receptors. Heightened expressions of these proteins have been linked to different pathological conditions.[52] The other upregulated proteins were a Rous sarcoma virus transcription enhancer factor II and a clathrin light chain A protein, both of which can increase the cell's susceptibility to microbial invasions.

In conclusion, our results show that PMA downregulates mitochondrial function, impairs energy metabolism and nuclear functions of the enterocytes such as their transcriptional and translational activities, and disrupts cytoskeletal homeostasis and focal adhesion which most likely contribute to cellular dystrophy, cachexia, and distension of intercellular spaces. Extrapolating it to an in vivo situation, such changes in enterocytes can inevitably increase intestinal permeability and cause epithelial damage resulting in enteropathy. The PMA-induced changes in enterocytes may help understand the "leaky-gut" problem which is linked to several avian intestinal diseases.

Author Contributions
NCR and RL conceived and designed the experiment; AG, RL, and NCR carried out the experiment; and NCR and RL wrote the manuscript along with JOL.

Supplemental Material
Supplemental material for this article is available online.

ORCID iD
Narayan C Rath https://orcid.org/0000-0002-3697-4304

REFERENCES
1. Arrieta MC, Bistritz L, Meddings JB. Alterations in intestinal permeability. *Gut*. 2006;55:1512–1520.
2. Mu Q, Kirby J, Reilly CM, Luo XM. Leaky gut as a danger signal for autoimmune diseases. *Front Immunol*. 2017;8:598.

3. Quigley EM. Leaky gut—concept or clinical entity? *Curr Opin Gastroenterol*. 2016;32:74–79.

4. Smyth JA. Pathology and diagnosis of necrotic enteritis: is it clear-cut? *Avian Pathol*. 2016;45:282–287.

5. McDevitt R, Brooker J, Acamovic T, Sparks N. Necrotic enteritis: a continuing challenge for the poultry industry. *World Poultry Sci J*. 2006;62:221–247.

6. Rath NC, Liyanage R, Gupta A, Packialakshmi B, Lay JO Jr. A method to culture chicken enterocytes and their characterization. *Poult Sci*. 2018;97:4040–4047.

7. Goel G, Makkar HP, Francis G, Becker K. Phorbol esters: structure, biological activity, and toxicity in animals. *Int J Toxicol*. 2007;26:279–288.

8. Newton AC. Protein kinase C: perfectly balanced. *Crit Rev Biochem Mol Biol*. 2018;53:208–230.

9. Roffey J, Rosse C, Linch M, Hibbert A, McDonald NQ, Parker PJ. Protein kinase C intervention: the state of play. *Curr Opin Cell Biol*. 2009;21:268–279.

10. Marshall G, Kinghorn A. Short-chain phorbol ester constituents of croton oil. *J Am Oil Chem Soc*. 1984;61:1220–1225.

11. Awad WA, Hess C, Hess M. Enteric pathogens and their toxin-induced disruption of the intestinal barrier through alteration of tight junctions in chickens. *Toxins (Basel)*. 2017;9:E60.

12. Berin MC, Buell MG. Phorbol myristate acetate ex vivo model of enhanced colonic epithelial permeability. *Dig Dis Sci*. 1995;40:2268–2279.

13. Hecht G, Robinson B, Koutsouris A. Reversible disassembly of an intestinal epithelial monolayer by prolonged exposure to phorbol ester. *Am J Physiol*. 1994;266:G214–G221.

14. Tepperman BL, Soper BD, Chang Q, Brown JF, Wakulich CA. The effect of protein kinase C activation on colonic epithelial cellular integrity. *Eur J Pharmacol*. 2000;389:131–140.

15. Wang X, Lan M, Wu HP, et al. Direct effect of croton oil on intestinal epithelial cells and colonic smooth muscle cells. *World J Gastroenterol*. 2002;8:103–107.

16. Kannan L, Liyanage R, Lay J Jr, Packialakshmi B, Anthony N. Identification and structural characterization of avian beta-defensin 2 peptides from pheasant and quail. *J Proteomics Bioinform*. 2013;6:31–37.

17. Packialakshmi B, Liyanage R, Lay JO Jr, Makkar SK, Rath NC. Proteomic changes in chicken plasma induced by salmonella typhimurium lipopolysaccharides. *Proteomics Insights*. 2016;7:1–9.

18. Makkar S, Liyanage R, Kannan L, Packialakshmi B, Lay JO Jr, Rath NC. Chicken egg shell membrane associated proteins and peptides. *J Agric Food Chem*. 2015;63:9888–9898.

19. Searle BC. Scaffold: a bioinformatic tool for validating MS/MS-based proteomic studies. *Proteomics*. 2010;10:1265–1269.

20. Zheng Y. Fatty acid-binding proteins at a glance. *Protein Pept Lett*. 2014;21:572–577.

21. Smathers RL, Petersen DR. The human fatty acid-binding protein family: evolutionary divergences and functions. *Hum Genomics*. 2011;5:170–191.

22. Glatz JF, Storch J. Unravelling the significance of cellular fatty acid-binding proteins. *Curr Opin Lipidol*. 2001;12:267–274.

23. Dominiczak MH, Caslake MJ. Apolipoproteins: metabolic role and clinical biochemistry applications. *Ann Clin Biochem*. 2011;48:498–515.

24. Gajda AM, Storch J. Enterocyte fatty acid-binding proteins (FABPs): different functions of liver and intestinal FABPs in the intestine. *Prostaglandins Leukot Essent Fatty Acids*. 2015;93:9–16.

25. Furuhashi M, Saitoh S, Shimamoto K, Miura T. Fatty Acid-Binding Protein 4 (FABP4): pathophysiological insights and potent clinical biomarker of metabolic and cardiovascular diseases. *Clin Med Insights Cardiol*. 2014;8:23–33.

26. Bottasso Arias NM, Garcia M, Bondar C, et al. Expression pattern of fatty acid binding proteins in celiac disease enteropathy. *Mediators Inflamm*. 2015;2015:738563.

27. Levy E, Menard D, Delvin E, et al. Localization, function and regulation of the two intestinal fatty acid-binding protein types. *Histochem Cell Biol*. 2009;132:351–367.

28. Li G, Yang H, Li W, et al. Transcriptional suppression of human apolipoproteinA4 and apolipoproteinC3 genes by phorbol myristate acetate in hepatic and intestinal cells. *Biomed Mater Eng*. 2014;24:877–884.

29. Song JC, Rangachari PK, Matthews JB. Opposing effects of PKCalpha and PKCepsilon on basolateral membrane dynamics in intestinal epithelia. *Am J Physiol Cell Physiol*. 2002;283:C1548–C1556.

30. Lee E, Lee DH. Emerging roles of protein disulfide isomerase in cancer. *BMB Rep*. 2017;50:401–410.

31. Wu J, Liu T, Rios Z, Mei Q, Lin X, Cao S. Heat shock proteins and Cancer. *Trends Pharmacol Sci*. 2017;38:226–256.

32. Guzhova I, Margulis B. Hsp70 chaperone as a survival factor in cell pathology. *Int Rev Cytol*. 2006;254:101-149.

33. Li Z. Glucose regulated protein 78: a critical link between tumor microenvironment and cancer hallmarks. *Biochim Biophys Acta*. 2012;1826:13–22.

34. Srivastava P. Interaction of heat shock proteins with peptides and antigen presenting cells: chaperoning of the innate and adaptive immune responses. *Annu Rev Immunol*. 2002;20:395–425.

35. Radons J. The human HSP70 family of chaperones: where do we stand? *Cell Stress Chaperones*. 2016;21:379V404.

36. Dudeja V, Vickers SM, Saluja AK. The role of heat shock proteins in gastrointestinal diseases. *Gut*. 2009;58:1000–1009.

37. Xue LY, Agarwal ML, Varnes ME. Elevation of GRP-78 and loss of HSP-70 following photodynamic treatment of V79 cells: sensitization by nigericin. *Photochem Photobiol*. 1995;62:135–143.

38. Pratt WB, Gestwicki JE, Osawa Y, Lieberman AP. Targeting Hsp90/Hsp70-based protein quality control for treatment of adult onset neurodegenerative diseases. *Annu Rev Pharmacol Toxicol*. 2015;55:353–371.

39. Arnal ME, Lalles JP. Gut epithelial inducible heat-shock proteins and their modulation by diet and the microbiota. *Nutr Rev*. 2016;74:181–197.

40. Liedel JL, Guo Y, Yu Y, et al. Mother's milk-induced Hsp70 expression preserves intestinal epithelial barrier function in an immature rat pup model. *Pediatr Res*. 2011;69:395–400.

41. Kitamura H, Yamamoto S, Nakase H, et al. Role of heat shock protein 47 in intestinal fibrosis of experimental colitis. *Biochem Biophys Res Commun*. 2011;404:599–604.

42. Wynn TA, Ramalingam TR. Mechanisms of fibrosis: therapeutic translation for fibrotic disease. *Nat Med*. 2012;18:1028–1040.

43. Keller HU, Niggli V, Zimmermann A. Diacylglycerols and PMA induce actin polymerization and distinct shape changes in lymphocytes: relation to fluid pinocytosis and locomotion. *J Cell Sci*. 1989;93:457–465.

44. Larsson C. Protein kinase C and the regulation of the actin cytoskeleton. *Cell Signal*. 2006;18:276–284.

45. Kouloukoussa M, Aleporou-Marinou V, Angelopoulou B, et al. Phorbol myristate acetate induces changes on F-actin and vinculin content in immature rat Sertoli cells. *Tissue Cell*. 2004;36:149–155.

46. Khalili AA, Ahmad MR. A review of cell adhesion studies for biomedical and biological applications. *Int J Mol Sci*. 2015;16:18149–18184.

47. Hayashi M, Ninomiya Y, Hayashi K, Linsenmayer TF, Olsen BR, Trelstad RL. Secretion of collagen types I and II by epithelial and endothelial cells in the developing chick cornea demonstrated by in situ hybridization and immunohistochemistry. *Development*. 1988;103:27–36.

48. Perche O, Hayashi M, Hayashi K, Birk D, Trelstad RL, Sandoz D. Origin of type I collagen localized within oviduct epithelium of quail hyperstimulated by progesterone. *J Cell Sci*. 1990;95:85–95.

49. Hilska M, Collan Y, Peltonen J, Gullichsen R, Paajanen H, Laato M. The distribution of collagen types I, III, and IV in normal and malignant colorectal mucosa. *Eur J Surg*. 1998;164:457–464.

50. Graham MF, Diegelmann RF, Elson CO, et al. Collagen content and types in the intestinal strictures of Crohn's disease. *Gastroenterology*. 1988;94:257–265.

51. DiGiacomo V, Meruelo D. Looking into laminin receptor: critical discussion regarding the non-integrin 37/67-kDa laminin receptor/RPSA protein. *Biol Rev Camb Philos Soc*. 2016;91:288–310.

52. Bridges D, Moorhead GB. 14-3-3 proteins: a number of functions for a numbered protein. *Sci STKE*. 2005;2005:re10.